

DESIGN AND EXPERIMENT OF MULTI-FRUIT GRIPPING AND CUTTING LINKAGE KIWIFRUIT PICKING END-EFFECTOR

多果夹持切割联动式猕猴桃采摘末端执行器设计与试验

Min FU*, Jianan CAI, Shike GUO, Lei CHEN, Chengmeng WANG, Gangqiang YANG, Xiaoman CUI

Northeast Forestry University, College of Mechanical and Electrical Engineering, Harbin / China;

Tel: +86 15663688203; E-mail: fumin1996@163.com

DOI: <https://doi.org/10.35633/inmateh-72-63>

Keywords: kiwifruit; picking end-effector; cluster; gripping and cutting linkage

ABSTRACT

Kiwifruit picking robots can replace manual labor for mechanized kiwifruit harvesting. However, existing picking robots encounter issues such as low separation efficiency of fruit stalks, poor stability of fruit gripping, and inaccurate identification when picking kiwifruit clusters. In response, a multi-fruit picking end-effector was designed to pick clusters of kiwifruit efficiently based on their distribution characteristics. The gripping range of the gripping device was determined based on the parameters of the spatial distribution of the fruit clusters. A multi-fruit gripping mechanics model was constructed, and the gripping force was analyzed to ensure efficient and stable fruit picking. Critical parameters of the fruit stalk separation device were determined through kinematic trajectory analysis to improve the separation efficiency of fruit stalks. Additionally, a dual-sensor fusion recognition method was proposed to identify fruit cluster locations accurately. The results of the picking experiment demonstrate that the end-effector can pick fruits in an average time of 8.28 s per cluster, with a net fruit-picking rate of 87.5% and a fruit damage rate of 7.5%. The end-effector shows a positive picking effect on kiwifruit fruits distributed in clusters. This study can serve as a reference for the development of kiwifruit-picking robots.

摘要

猕猴桃采摘机器人可替代人工劳作实现猕猴桃机械化收获。但现有采摘机器人采摘成簇分布猕猴桃时，末端执行器存在果梗分离效率低、果实夹持稳定性差、果实识别准确度低等问题。对此，本文根据猕猴桃果实的分布特征，设计了一种多果夹持切割联动式采摘末端执行器，以期实现成簇果实的快速采摘作业。根据果实簇空间分布参数确定夹持装置夹持范围，构建多果稳定夹持力学模型并对夹持力进行分析，基于运动学轨迹分析确定果梗剪切装置关键参数。在此基础上，提出了一种双传感器融合识别方法以实现果实簇位置的准确判别。采摘试验结果表明该末端执行器采摘每簇果实平均时间为 8.28s，果实净采摘率为 87.5%，果实损伤率为 7.5%，对簇生分布的猕猴桃果实有良好采摘效果。该研究可为猕猴桃采摘机器人研制提供参考。

INTRODUCTION

Kiwifruit was a highly economical fruit and was still mainly picked manually at a high cost, which was desirable for mechanical harvesting (Fang et al., 2023). With the rapid growth of the kiwifruit industry and its global production expected to double by 2025, manual harvesting cannot meet current market demand (Au et al., 2022; Li et al., 2022). The efficacy of the end-effector, as a terminal device in direct contact with the fruit, plays a crucial role in the performance of a picking robot in terms of versatility, practicality, and picking efficiency (Bu et al., 2020).

According to the working principle, the end-effector can be divided into three types: gripping, envelope and adsorption (Lan et al., 2022). Fruit stalk separation methods include pulling, cutting, and twisting. For instance, Zhi et al. designed a gripping kiwifruit-picking end-effector with bionic fingers that grip the fruits, leading to the separation of the fruit and the stalk as the end-effector rotates. Despite its simple structure, the rotating process of this end-effector can cause damage to neighboring fruits (Zhi et al., 2023). Similarly, Fu et al. designed a multi-fruit cutting kiwifruit picking end-effector, which allows for the aggregation of fruit clusters into the picking bin interior through an envelope and the cutting of stalks with a rotary cutter, resulting in enhanced harvesting efficiency through cluster harvesting methods. However, the rotary cutter unit of this end-effector was large and inflexible (Fu et al., 2023).

In another development, Wang et al., designed an apple-picking end-effector with bionic suction cups, featuring four evenly distributed suction cups on the manipulator that utilize negative vacuum pressure to produce concave deformation, enabling the cups to fit the apple's surface and adsorb it. The fruit stalk was separated through wrist rotation and dragging in a compound manner, making this picking method adaptable to different fruit shapes but suitable only for fruits with smooth surfaces (Wang et al., 2022). To improve the successful rate of fruit picking, Zhang et al. equipped the cherry tomato picking end-effector with Intel's RealSense D415 depth camera mounted on the side of the robotic arm base to facilitate unobstructed tomato harvesting (Zhang et al., 2021). Similarly, Yu et al. utilized the DF810-HD depth camera to support the picking robot visually during tomato picking (Yu et al., 2022). However, it was essential to note that a single recognition sensor may need help to adapt to complex and changing harvesting environments. In addressing this challenge, Sarabu et al. devised a dual-arm picking end-effector, each arm equipped with an RGB-D depth camera, to enhance fruit recognition efficiency through cross-view recognition. Nonetheless, the high cost of the equipment poses a challenge to widespread adoption (Sarabu et al., 2019).

The studies outlined above have significantly informed the development of fruit-picking robots for kiwifruit and other fruits. However, the focus of previous research on end-effector has been predominantly on single-fruit picking. This limitation has led to several issues when harvesting kiwifruit distributed in clusters, such as lack of stability when gripping fruits, easy fruit detachment, and damage caused by twisting or pulling during separation from the stalks. Furthermore, using a single visual recognition sensor with low precision has also affected picking efficiency (Jin et al., 2022). In response to these challenges, this paper has addressed the issues above by designing a multi-fruit gripping and cutting linkage end-effector based on the characteristics of kiwifruit cluster distribution. This end-effector enables the synchronization of fruit gripping and stalk separation processes, ultimately leading to efficient harvesting of fruit clusters. Additionally, a prototype was fabricated, and a kiwifruit picking test bed was built to verify the effectiveness of this end-effector. The research results from this study can offer valuable insights for improving the efficiency of cluster fruit picking and reducing the rate of fruit damage.

MATERIALS AND METHODS

Kiwifruit distribution characteristics

Kiwifruit large-scale planting was usually carried out using a trellis planting mode, with an average row spacing of 4 m, a spacing of 2 m between trellis columns, and an average trellis height of 2 m, the fruits were distributed in a spatial range of 1.5 to 1.8 m in height from the ground, as shown in Figure 1(a). Kiwifruit hang down from the branches and were found in clusters, which come in three types: single fruit, linear cluster, and aggregation cluster, as shown in Figure 1(b). Notably, a single fruit was not surrounded by neighboring fruits, while a linear cluster typically consists of 1-2 fruits distributed on either side of the central fruit. Additionally, a maximum of two adjacent fruits can be found per fruit. The fruits within aggregation clusters display irregular distribution and usually comprise 4-6 fruits (Ma et al., 2022).

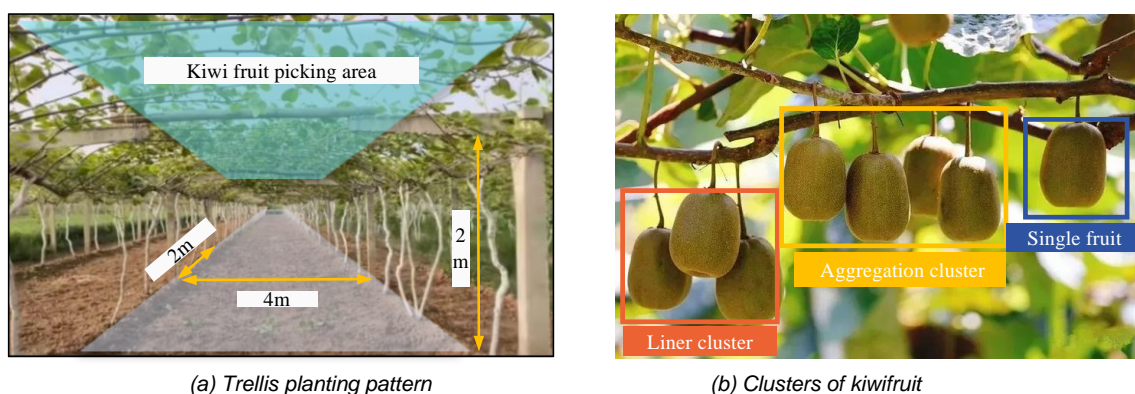


Fig. 1 - Environment for planting kiwifruit fruits

The spatial distribution of kiwifruit fruit in the picking area affects the efficiency of the end-effector picking operation (Li et al., 2022). To ensure the picking success rate of the end-effector, the spatial distribution parameters of "Hongyang" kiwifruit in Nanjing Lile Agricultural Planting Base were analyzed as an example to provide a basis for the design of the end-effector for picking, as shown in Figure 2.

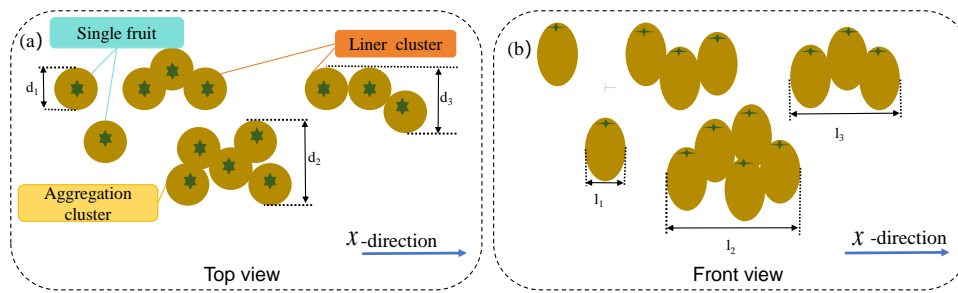


Fig. 2 - Spatial distribution of kiwifruit

Single fruit distribution length was d_1 and width was l_1 ; aggregation cluster distribution length d_2 , distribution width l_2 ; linear cluster distribution length d_3 , distribution width l_3 . Fifteen groups were randomly selected for each growth state for the measurement of their physical parameters, the measured data can be found in Table 1.

Table 1

Spatial distribution parameters of kiwifruit						
Numerical value	Single fruit length d_1 [mm]	Single fruit width l_1 [mm]	Aggregation cluster length d_2 [mm]	Aggregation cluster width l_2 [mm]	Linear cluster length d_3 [mm]	Linear cluster width l_3 [mm]
maximum value	60.5	40.48	72.12	181.42	83.36	138.79
minimum value	52.3	31.26	65.23	171.23	79.21	129.41
Range	8.3	9.22	6.89	10.19	4.15	9.38
Average value	55.6	43.23	68.91	178.56	81.42	132.45

Overall structure and working principle of the end-effector

A multi-fruit gripping and cutting linkage end-effector was designed to target kiwifruit clusters' distribution characteristics, and the structure schematic was shown in Figure 3. The end-effector mainly comprises a movable gripping plate, a fixed gripping plate, a cutter, a stepper motor, a crank-rocker mechanism, and two identification sensors. A stepper motor was used as the power output. In addition, lightweight 3D printing materials were utilized in fabricating the entire machine, except the cutter and crank-rocker mechanism, ensuring the overall structure was light.

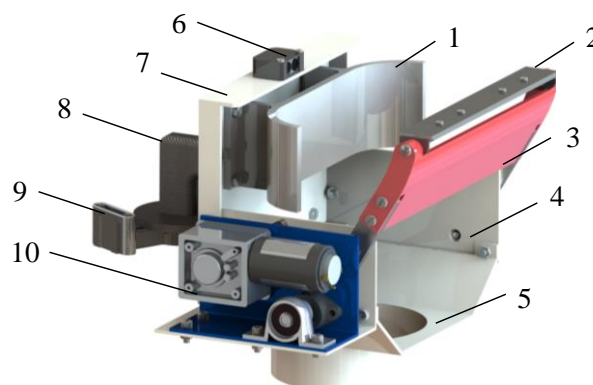


Fig. 3 - End-effector structure

1.fixed gripping plate; 2.cutter; 3 movable gripping plate; 4.sidewall plate; 5.collection cylinder; 6.color recognition sensor; 7.back plate; 8.flange holder; 9.binocular camera; 10.motor module

The working principle of the kiwifruit picking system was illustrated in Figure 4. Firstly, the end-effector was moved to the kiwifruit picking area by a robotic arm, followed by a binocular camera upward scanning the kiwifruit clusters, the target clusters were identified by clustering, and the coordinate information was acquired. Subsequently, the robotic arm elevates the end-effector to match the obtained fruit cluster coordinates for enveloping the fruit. The robotic arm stops moving when the color recognition sensor detects that all fruits have entered the fruit-gripping device. The cutter and the movable gripping plate rotate to synchronize the completion of the fruit gripping and cutting the fruit stalk action. The fruit then smoothly transitions into the fruit collection end, completing the single-picking process as it slides along the end-effector sidewall panel.

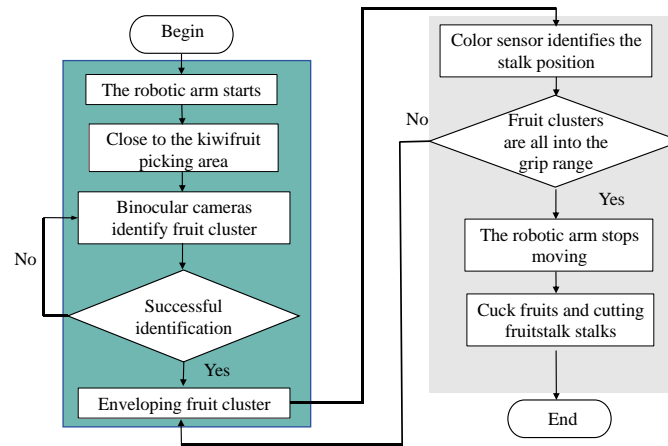


Fig. 4 - Working Principle

Parameter design of the fruit gripping device

The structure of the fruit-gripping device was illustrated in Figure 5(a). It consists of two parts: the movable and fixed gripping plates. The movable gripping plate was mounted on the crank rocker device, driven by the stepping motor, the movable gripping plate counterclockwise rotation with the fixed gripping plate to achieve a cluster of fruit stable fixture. The kiwifruit's spatial distribution parameters determined the gripping area dimensions. The design of the movable gripping plate was 160 mm in length and 45 mm in height, and the fixed gripping plate is 180 mm in length and 52 mm in height. When the gripping device comes into contact with fruit clusters, the fruits' positions may shift, resulting in a sliding zone within the 6.9-9.1 mm range from the center to the edge (Williams et al., 2020), as shown in Figure 5(b). This sliding zone could cause the gripping device to collide with neighboring fruits, leading to fruit drop. To mitigate this issue, the edges of both gripping plates were designed to be curved, guiding the target fruit clusters into the interior of the gripping device. This design effectively reduces the sliding zone and minimizes the risk of collision with neighboring fruits, ensuring a stable grip on the fruit cluster.

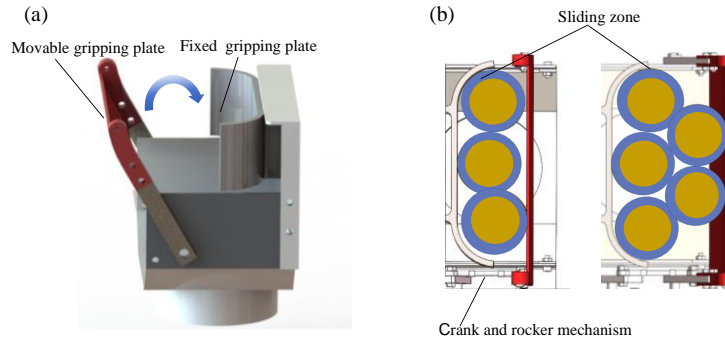


Fig. 5 - Fruit gripping device structure

To ensure the stability of the gripping device when gripping multiple fruits, it was essential to maintain an adequate gripping force. However, it was important to avoid applying excessive force that may damage the fruits during the gripping process. Therefore, it was necessary to establish a multi-fruit gripping mechanical model to determine the appropriate range of gripping force, thus ensuring both stability and the prevention of fruit damage, as shown in Figure 6.

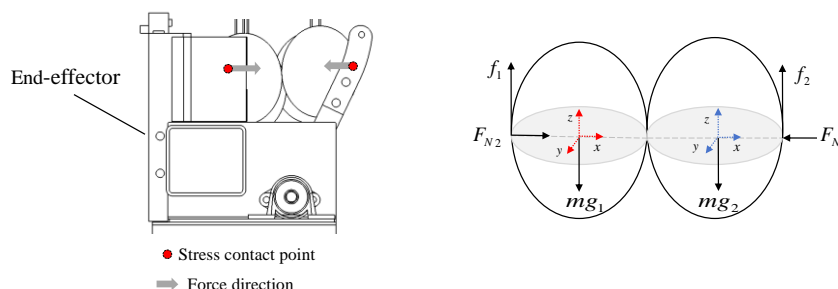


Fig. 6 - Multi-fruit gripping mechanical model

The fact that the fruit does not fall in the vertically straight direction and does not undergo relative sliding in the horizontal direction should be satisfied:

$$\begin{cases} f_1 + f_2 = mg_1 + mg_2 \\ f_1 = \mu F_{N1} \\ f_2 = \mu F_{N2} \\ F_{N1} = F_{N2} \end{cases} \quad (1)$$

where:

F_{N1} was the gripping force generated by the movable gripping plate, F_{N2} was the support force generated by the fixed gripping plate, f_1, f_2 was the maximum static friction in the perpendicular direction, mg_1, mg_2 was the gravitational force of the fruit itself, μ was the coefficient of friction.

To avoid fruit damage, the gripping force provided to the kiwifruit by the gripping plate should also satisfy.

$$\frac{mg_1 + mg_2}{2\mu} \leq F_{N1} \leq F_b \quad (2)$$

where:

F_b was the destructive force suffered by the fruit damage, and according to the literature (Dong et al., 2022), the effective gripping force for the fruit not to slip is not less than 1.08 N. The kiwifruit shows significant internal damage to the pulp tissue, at which point the fruit is subjected to destructive forces in the range of 10-15 N. Considering the clamping stability and gripping damage, the preset gripping force should be between 1.08-15 N.

Design of the fruit stalk separation device

Kiwifruit stalks and fruit at the combination of the separation layer of tissue were susceptible to shear shedding (Silwal et al., 2021). According to the shedding characteristics of the separated layer of the fruit, a cutting fruit stalk separation device was designed as shown in Figure 7(a). The cutter was fitted on the movable gripping plate, driven by a stepping motor, to complete the operation of gripping the fruit and cutting off the stalks in turn, as shown in Figure 7(b).

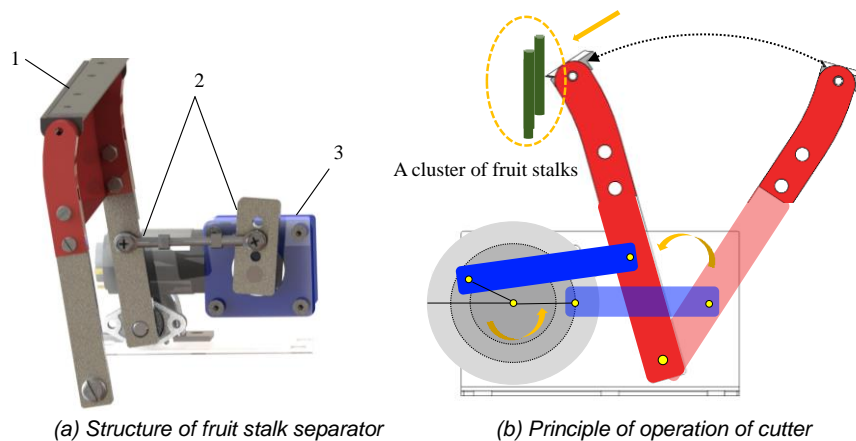


Fig. 7 - Structure and working principle of the fruit stalk separator
1. Cutter; 2. Crank rocker assembly; 3. Stepper motor

When the fruit stalk separating device was in motion, it was essential to ensure a smooth fruit stalk separating process and prevent the fruit from falling off vibrations. Accordingly, a crank-rocker mechanism without sharp return characteristics was designed, and its kinematic analysis was shown in Figure 8.

The angle between the limit positions of cranks AB_1 and AB_2 was 0° , and the rocker reaches two limit positions, F_1 and F_2 , during its movement. F_1 ensures that the cutter can cut the stalks sufficiently, and F_2 provides enough space between the movable and fixed gripping, the angle swept by DF_1 and DF_2 was the range of motion of the cutter.

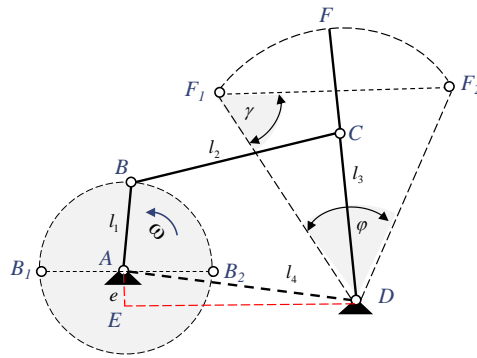


Fig. 8 - Kinematic analysis of the crank rocker mechanism

A, B, C, D indicates the crank rocker mechanism connection point; F indicates the rocker extension point; E indicates the intersection of the horizontal projection direction of the frame and the vertical projection direction; B₁, B₂ is the limit position point of the crank; C₁, C₂ is the limit position point of the rocker extension direction

According to the mechanism characteristics of the crank rocker without emergency return, it can be obtained that:

$$\begin{cases} \sin \frac{\varphi}{2} = \frac{l_1}{l_3} \\ l_1^2 + l_4^2 = l_2^2 + l_3^2 \\ e = l_3 \cdot \sin \left(\frac{\pi}{2} - \frac{\varphi}{2} \right) \end{cases} \quad (3)$$

where:

l_1 indicates crank length, mm; l_2 indicates the length of connecting rod, mm; l_3 indicates the length of rocker, mm; l_4 indicates the length of frame, mm; l_4 was the horizontal projection length of frame, mm.

The crank length l_1 was calculated from Equation 3 to be 45 mm. In crank-rocker mechanism, the transmission angle γ is used to measure the force transmission performance of the mechanism. The permissible transmission angle γ is generally 40° to 50° (El-Shakery et al., 2021). Larger values of γ indicate better force transfer performance. In the absence of rapid return motion, the minimum transmission angle occurs γ_{min} at two positions where the crank and frame lines coincide, and the transmission angles at the two positions were equal. This can be obtained by combining with Equation 1:

$$\begin{cases} \gamma = \arccos \frac{l_1 l_4}{l_2 l_3} \\ l_4 = \sqrt{460 + l_2^2} \\ \gamma_{min} = \arccos \frac{\sqrt{460 + l_2^2}}{l_2^2} \end{cases} \quad (4)$$

The transmission angle γ rises sharply as l_2 increases and then tends to 60°, the longer the connecting link, the more the mass of the transmission mechanism increases. If the length is increased after 65 mm, the minimum transmission angle does not increase significantly, in order to ensure the compactness of the machine, $l_2=65$ mm, $l_3=40$ mm the minimum transmission angle at this point is 53.7°, which meets the transmission performance requirements.

Design of the fruit identification devices

The paper proposes a dual visual recognition sensor fusion method to enhance the accuracy of fruit cluster recognition during the picking phase, mainly focusing on the shape and color characteristics of kiwifruits. Initially, a binocular vision camera was mounted at the base of the end-effector to capture the spatial coordinates of kiwifruit clusters by identifying their centers at the bottom. Subsequently, the robotic arm manipulates the end-effector based on these coordinates to encase the target fruit clusters, thereby effectively averting shading between clusters and obviating interference from branches and leaves. The working principle of this process was depicted in Figure 9(a). Once all the fruit clusters were inside the gripper, the green fruit stalks were positioned above the gripping plate. A color sensor detects the green color, and the robotic arm stops moving when it detects a green signal from the fruit stalk, as illustrated in Figure 9(b). This integrated sensor fusion method ensures precise and efficient recognition of fruit clusters during the picking process.

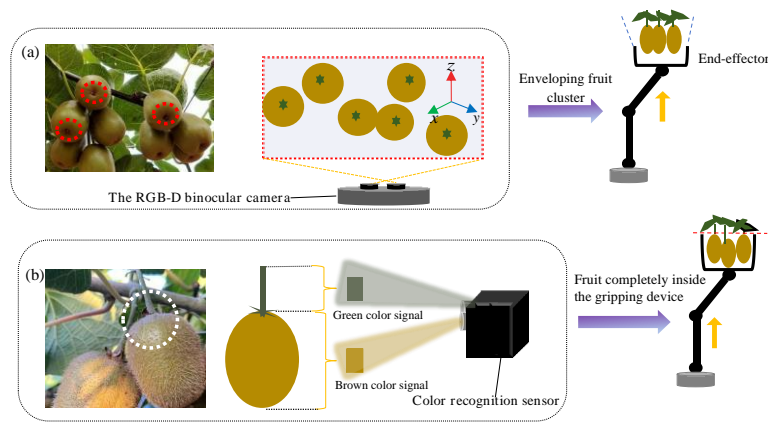


Fig. 9 - Working principle of the identification device fruit

Experimental condition

The experiment simulated a kiwifruit trellis seeding environment and was conducted in the Robotics Laboratory of the School of Mechanical and Electrical Engineering, Northeast Forestry University. The principal experimental equipment comprised a planting trellis, end-effector, AUBO-E5 robotic arm experimental bench, LegionY7000P computer, and collection device, as shown in Figure 10.

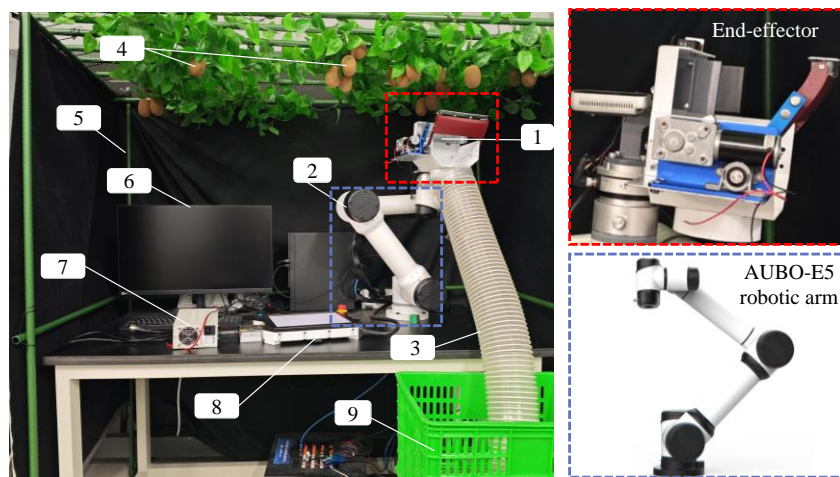


Fig. 10 - Experimental environment

1. end-effector; 2. robotic arm; 3. hose; 4. kiwifruit; 5. trellis; 6. desktop computer; 7. mobile power supply; 8. control panel; 9. collection box

Test method

The picking experiment was conducted on December 15, 2023, and the AUBO-E5 robotic arm was used to assist the end-effector in picking. 80 randomly selected kiwifruit of different shapes were used for the picking experiment to verify end-effector harvesting performance. According to the distribution characteristics of kiwifruit fruit clusters, in order to ascertain the effect of the end-effector on the picking of different types of kiwifruit fruit clusters, 80 kiwifruit were divided into 5 groups, each containing 5 clusters of the same number of fruits. Single-fruit clusters contain one fruit, linear clusters contain 2 and 3 fruits, and aggregated clusters have several 4 and 6 fruits. The average picking time per cluster, the net fruit picking rate, and the fruit damage rate are used as the evaluation indexes for fast and damage-free picking. It is defined as follows:

$$\begin{cases} P_T = t_1 - t_0 / 5 \\ P_C = n_1 / n_2 \times 100\% \\ P_D = m_1 / n_2 \times 100\% \end{cases} \quad (5)$$

where:

P_T was the average picking time per cluster, t_0 was the start time of the robotic arm driving the end-effector to reach the kiwifruit picking area. t_1 was the end time until the fruits fall into the collection device, P_C was the net fruit picking rate, n_1 was the number of harvested fruits, n_2 was the number of fruits in the picking area, and P_D was the fruit damage rate, m_1 was the number of fruits damaged by picking.

RESULTS

Picking experiments were carried out on 5 groups of 3 types of fruit clusters, and the harvesting process was shown in Figure 11. The robotic arm moves the end-effector to the fruit picking area and determines the position of the fruit by means of dual-sensor fusion recognition, after which the end-effector envelops the fruit upwards driven by the robotic arm. Subsequently, under the cooperation of the fruit gripping and fruit stalk separating device, the synchronized completion of the gripping of the fruit and cutting off the fruit stalk action, the fruit falls into the collection end. After picking, the robotic arm moved to the next picking target for picking operations.

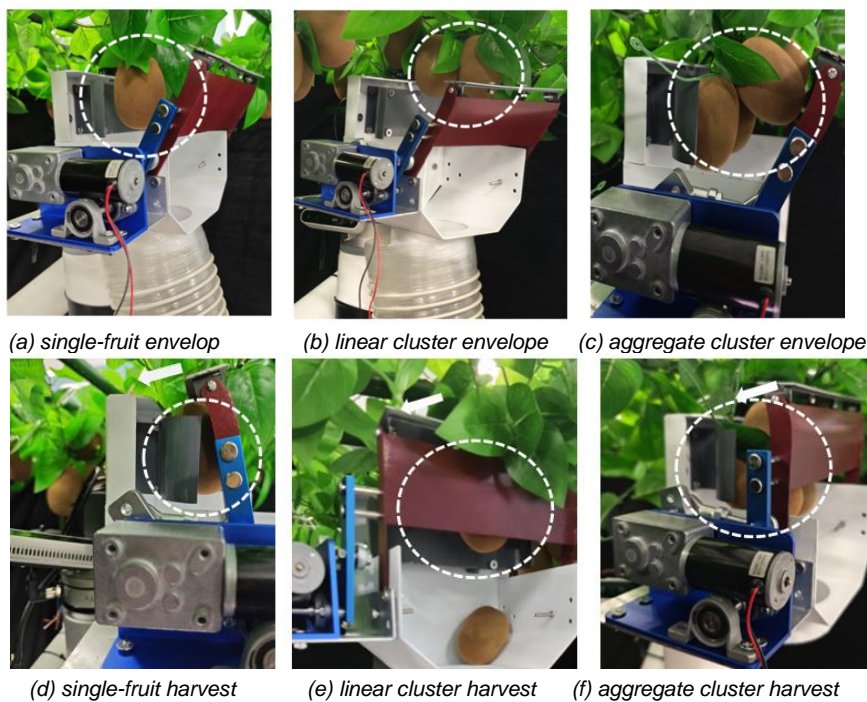


Fig. 11 - End-effector picking process

The results of the harvesting experiment were shown in Table 2.

Table 2

Results of picking experiments									
Type	Number of fruits	Number of fruit clusters	Total number of fruits	Number of fruits picked	Number of failed picks	Number of fruit damage	Average picking time per cluster (s)	Net picking rate (%)	Fruit damage rate (%)
Single-fruit	1	5	5	5	0	0	6.2	100	0
Linear cluster	2	5	10	10	0	0	7.1	100	0
	3	5	15	13	1	1	7.5	86.6	6.7
Aggregate cluster	4	5	20	17	1	2	9.2	85	10
	6	5	30	25	2	3	11.4	83.3	10
Total		20	80	70	4	6	9.48	87.5	7.5

As shown in Table 3, the average picking time per cluster was 8.28 seconds, the net fruit picking rate was 87.5%, and the fruit damage rate was 7.5%. Meanwhile, the net picking rate for a single fruit was 100%, and the fruit damage rate was 0. According to the literature (Mu et al., 2021), the linear cluster type of fruit distribution occupies about 87% of the picking area, and the end-effector achieves an average net picking rate of 93.3% for this type of fruit cluster. The net picking rate was 100% for linear clusters with two fruits, and the fruit damage rate was 0. The net fruit picking rate for linear clusters with three fruits was 86.6%, and the fruit damage rate was 6.7%. The aggregated cluster picking operation with four and six fruits also had a net picking rate of 84.14%. Still, there was an increasing trend in the fruit destruction rate and a significant increase in the average picking time per cluster when picking aggregated cluster distribution fruit.

In summary, the designed end-effector provides excellent harvesting results for all three types of kiwifruit clusters, especially for kiwifruit distributed in single and linear clusters. Capable of meeting the current demand for kiwifruit picking in clusters. The main reason for the increase in fruit damage was that the cutter was interfered with by kiwifruit vines, which scratched the surface of the fruit. The rise in the average picking time per cluster was due to the excessive number of fruits and their disorganized distribution, which reduces the recognition efficiency of the fruit identification device.

CONCLUSIONS

(1) Aiming to address the distribution characteristics of kiwifruit fruit clusters, a multi-fruit gripping and cutting linkage picking end-effector was designed, which integrates the fruit stalk separating and fruit gripping devices, linking the gripping of fruits with the cutting of fruit stalk, simplifying the structure and improving the picking efficiency. Moreover, proposing a dual-sensor fusion recognition method enhances the accuracy of fruit cluster identification. It mitigates the impact of environmental factors on the selection of different types of kiwifruit clusters.

(2) The picking experiment showed that the end-effector picked each cluster of fruits in an average time of 8.28 s, with a net fruit picking rate of 87.5% and a fruit damage rate of 7.5%. It has a net picking rate of 93.3% for kiwifruit fruits in linear clusters with the widest distribution area, and at the same time, it has good picking effect for kiwifruit fruits distributed in single and aggregated clusters, with high picking adaptability, which can meet the current demand of mechanized picking.

ACKNOWLEDGEMENT

This paper was funded by the National Natural Science Foundation of China (Grant No.51975114).

REFERENCES

- [1] Au, C. K., Redstall, M., Duke, M., Kuang, Y. C., & Lim, S. H. (2022). Obtaining the effective gripper dimensions for a kiwifruit harvesting robot using kinematic calibration procedures. *Industrial Robot: the international journal of robotics research and application*, 49(5), 865-876.
- [2] Bu, L. X., Chen, C. K., Hu, G. R., Sugirbay, A., & Chen, J. (2020). Technological development of robotic apple harvesters: A review. *INMATEH-Agricultural Engineering*, 61(2), 151-164.
- [3] Dong Z Y. (2022) *Research on kiwi fruit picking technology and device based on machine vision and parallel mechanical arm (基于机器视觉与并联机械臂的猕猴桃采摘技术及装置研究)* [Thesis of Master, Northwest Agriculture and Forestry University]. China Campus Repository.
- [4] El-Shakery, S., Ramadan, R., & Khader, K. (2020). Analytical and Graphical Optimal Synthesis of Crank-Rocker Four Bar Mechanisms for Achieving Targeted Transmission Angle Deviations. *Jordan Journal of Mechanical & Industrial Engineering*, 14(3).
- [5] Fang, W., Wu, Z., Li, W., Sun, X., Mao, W., Li, R., & Fu, L. (2023). Fruit detachment force of multiple varieties kiwifruit with different fruit-stem angles for designing universal robotic picking end-effector. *Computers and Electronics in Agriculture*, 213, 108225.
- [6] Ji, W., Huang, X., Wang, S., & He, X. (2023). A Comprehensive Review of the Research of the "Eye-Brain-Hand" Harvesting System in Smart Agriculture. *Agronomy*, 13(9), 2237.
- [7] Li, M., & Liu, P. (2023). A bionic adaptive end-effector with rope-driven fingers for pear fruit harvesting. *Computers and Electronics in Agriculture*, 211, 107952.
- [8] Li, K., Huo, Y., Liu, Y., Shi, Y., He, Z., & Cui, Y. (2022). Design of a lightweight robotic arm for kiwifruit pollination. *Computers and Electronics in Agriculture*, 198, 107114.
- [9] Lan, Y., Yan, Y., Wang, B., Song, C., & Wang, G. (2022). Current status and future development of the key technologies for intelligent pesticide spraying robots. *Trans. Chin. Soc. Agric. Eng*, 38, 30-40.
- [10] Min, F. U., Shike, G. U. O., Jianan, C. A. I., Jiacheng, Z. H. O. U., & Xiaoyi, L. I. U. (2023). TRIZ-aided design and experiment of kiwifruit picking end-effector. *INMATEH-Agricultural Engineering*, 71(3).
- [11] Ma, L., He, Z., Zhu, Y., Jia, L., Wang, Y., Ding, X., & Cui, Y. (2022). A Method of Grasping Detection for Kiwifruit Harvesting Robot Based on Deep Learning. *Agronomy*, 12(12), 3096.
- [12] Mu, L., Cui, G., Liu, Y., Cui, Y., Fu, L., & Gejima, Y. (2020). Design and simulation of an integrated end-effector for picking kiwifruit by robot. *Information Processing in Agriculture*, 7(1), 58-71.

- [13] Mu, L. (2019) *Full Field of View Information Perception and Integrated Picking Method for Kiwifruit Harvesting Robot* (猕猴桃收获机器人的信息感知与综合采摘方法研究) [Thesis of Master, Northwest Agriculture and Forestry University]. China Campus Repository.
- [14] Sarabu, H., Ahlin, K., & Hu, A. P. (2019, July). Graph-based cooperative robot path planning in agricultural environments. In 2019 *IEEE/ASME International Conference on Advanced Intelligent Mechatronics (AIM)*. pp. 519-525. IEEE.
- [15] Williams, H., Ting, C., Nejati, M., Jones, M. H., Penhall, N., Lim, J., & MacDonald, B. (2020). Improvements to and large-scale evaluation of a robotic kiwifruit harvester. *Journal of Field Robotics*, 37(2), 187-201.
- [16] Wang, M., Yan, B., Zhang, S., Fan, P., Zeng, P., Shi, S., & Yang, F. (2022). Development of a Novel Biomimetic Mechanical Hand Based on Physical Characteristics of Apples. *Agriculture*, 12(11), 1871.
- [17] Yu, F., Zhou, C., Yang, X., Guo, Z. H., & Chen, C. L. (2022). Design and Experiment of Tomato Picking Robot in Solar Greenhouse. *Transactions of the Chinese Society for Agricultural Machinery*, 53(1), 41-49.
- [18] Zhi, H. E., Zixu, L. I., Xingting, D. I. N. G., Kai, L. I., Yinggang, S. H. I., & Yongjie, C. U. I. (2023). Design and experiment of end effect for kiwifruit harvesting based on optimal picking parameters. *INMATEH-Agricultural Engineering*, 69(1).
- [19] Zhang, Q., Liu, F. P., Jiang, X. P., Xiong, Z., & Xu, C. (2021). Motion planning method and experiments of tomato bunch harvesting manipulator. *Transactions of the CSAE*, 39(7), 149-156.